



ELSEVIER

Contents lists available at ScienceDirect

Materialia

journal homepage: [www.elsevier.com/locate/mtla](http://www.elsevier.com/locate/mtla)

Full Length Article

## Using machining force feedback to quantify grain size in beta titanium

Daniel Suárez Fernández<sup>a,b,\*</sup>, M. Jackson<sup>a</sup>, P. Crawforth<sup>b</sup>, K. Fox<sup>c</sup>, B.P. Wynne<sup>a,d</sup><sup>a</sup> Department of Materials Science and Engineering, The University of Sheffield, Sir Robert Hadfield Building, Mappin St, Sheffield S1 3JD, UK<sup>b</sup> Advanced Manufacturing Research Centre, Advanced Manufacturing Park, Catcliffe, Rotherham S60 5TZ, UK<sup>c</sup> Rolls-Royce plc, PO Box 31, Derby DE24 8BJ, UK<sup>d</sup> Department of Mechanical and Aerospace Engineering, The University of Strathclyde, 75 Montrose St, Glasgow G1 1XJ, UK

## ARTICLE INFO

## Keywords:

Titanium alloys  
Machining  
Characterisation  
Forging  
Grain size

## ABSTRACT

The fluctuating forces on the cutting tool generated during machining of  $\beta$  processed Ti-17 alloy are shown to contain sufficient information to enable measurement of  $\beta$  grain size to an equivalent accuracy of standard etching methods. Three orthogonal forces were gathered, cutting force tangential to the rotation, the force in the feed (radial) direction, and the normal force in the longitudinal axis. Each individual force produced a microstructure image with a high level of contrast but in some cases did not fully highlight all features as shown in the optical image of the equivalent area. By normalising and combining the three forces into a vector, followed by noise reduction, a high-resolution image with sufficient detail to undertake grain size measurements using the linear intercept was produced. The measured grain size differed by no more than 5% with respect to the grain size measured in the etched micrograph. It is believed that the forces which have a higher proportion of elastic response in their total values, i.e., the feed and normal forces, produced the higher contrast images, indicating that elastic stresses produce the highest contrast between grains and plastic strains smear out the grain to grain variation.

## 1. Introduction

In the titanium manufacturing supply chain, particularly when supplying material for the aerospace industry, extensive and tedious materials testing is performed at intermediate stages of manufacture to assess the quality of the material before being sent for further downstream processing. These tests, such as chemical etching for grain size analysis, are extremely time and resource consuming, leading to only a few selected batches being selected for quality assessment. This work investigates the potential of measuring grain size in beta titanium alloys using the forces generated during machining, which if feasible could lead to a higher level of confidence in the quality of the final product as well as significant productivity improvements during manufacturing.

Large diameter billets (>100 mm) billets of aerospace quality titanium tend to be chemically homogeneous but can have a heterogeneous microstructure, owing to a complex non-linear deformation history experienced during cogging from the as-cast condition. Finite element modelling (FEM) has shown that cogging of Ti-64 ingot generates strains as high as 2 near the surface, decreasing to about 1 in the centre, directly impacting  $\beta$  grain size distribution and the fraction of globularised  $\alpha$  [1]. Crystallographic texture has also been shown to vary throughout the cross-section of Ti-834 billet using both electron backscattered and neutron diffraction [2].

Traditionally in machining studies of titanium, cutting force response has been used to determine the effect of cutting parameters on surface quality, tool wear, and the general health of the process [3–5]. In these analyses the material is considered to be isotropic and homogeneous and mean values of the cutting forces are considered sufficient. Hence, the effect of local variations and heterogeneities in the microstructure and macrostructure of the billet on the machining forces signals are not considered of any importance. However, recently Crawforth et al. [6] investigating the machinability of Ti-54M billet from the perspective of the lifetime of the cutting tool, noted that the cutting forces across the cross-section of the billet varied in proportion to the level of strain experienced in the cross-section, as predicted by FEM. It was hypothesised that this was due to the variations in microstructure and crystallographic texture induced because of the different strain paths experienced within the cross-section.

A small number of micromachining studies on single crystal material have investigated the effect of crystal orientation on cutting forces and machining induced damage. Yuan et al. [7] showed that during micromachining of single crystal aluminium the cutting forces and chip formation are dependent on the relationship between the crystallographic orientation and the cutting direction, for example, when cutting on the (110) plane the minimum and maximum forces were measured in the [001] and [110] directions, respectively. Lawson et al. [8], also using

\* Corresponding author at: Department of Materials Science and Engineering, The University of Sheffield, Sir Robert Hadfield Building, Mappin St, Sheffield S1 3JD, UK.

E-mail address: [D.Suarez@sheffield.ac.uk](mailto:D.Suarez@sheffield.ac.uk) (D. Suárez Fernández).

<https://doi.org/10.1016/j.mta.2020.100856>

Received 15 May 2020; Accepted 31 July 2020

Available online 11 August 2020

2589-1529/© 2020 Published by Elsevier B.V. on behalf of Acta Materialia Inc. This is an open access article under the CC BY license.

(<http://creativecommons.org/licenses/by/4.0/>)

**Table 1**  
Ti-17 chemical composition.

	Al	Sn	Zr	Mo	Cr
Min (w%)	4.5	1.6	1.6	3.5	3.5
Max (w%)	5.5	2.4	2.4	4.5	4.5

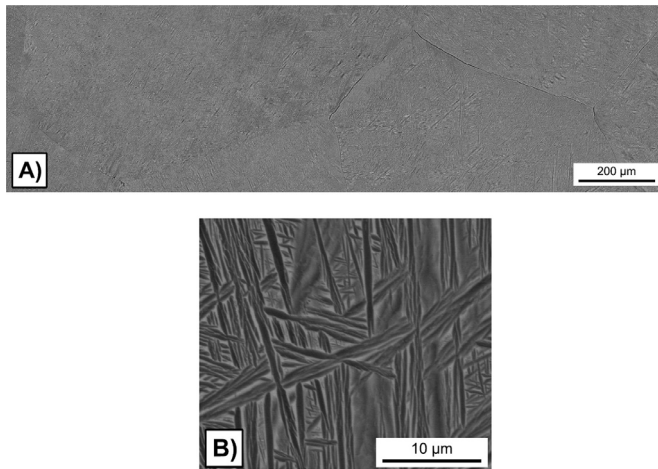


**Fig. 1.** SEM backscattered images of the Ti-17 analysed billet. (A) Detail of the prior beta grain boundaries and (B) detail of the basketweave lath geometry developed inside the prior beta grain structures.

aluminium single crystals, showed that the measured shear stress varied significantly as a function crystallographic orientation from 25 to 450 MPa. They also noted that the (320) plane, which had the highest specific cutting energy, had the lowest effective coefficient of friction, and therefore the lowest amount of energy expended for friction as compared to shearing. In contrast, the (670) plane had the lowest shear stress and the lowest specific cutting energy. Furthermore, Lee et al. [9] using face turning on single crystal copper material demonstrated that chip thickness and shear angle, as well as the as-machined surface roughness, was a function of crystal orientation. They found that surface roughness on average was greater when machining on the (110) and (111) planes than on the (100) plane and that there was more in-plane variation of roughness when machining in different directions on the (110) plane.

This paper reports on the further development of the concepts presented above, describing how cutting force measurements during machining can be used to characterise microstructure, in particular grain size in polycrystalline material, as long as the machining interaction volume is less than the effective structural unit size. This leads to the possibility of having an in-situ analysis technique to capture large scale grain size data that does not increase the manufacturing time but adds significant value to downstream processing and in-service performance prediction.

## 2. Experimental procedure

The material used in this investigation was a near-beta titanium alloy Ti-17 (Ti-5Al-2Sn-2Zr-4Mo-4Cr) billet, 117 mm in diameter, supplied in a beta processed condition by Timet UK Ltd. The general chemical composition of Ti-17 is shown in Table 1.

The as-received billet was processed above its beta transus temperature (890.5°C [10]) and water quenched. The microstructure consisted of large equiaxed  $\beta$  grains, 1360  $\mu\text{m}$  in diameter, Fig. 1(a), containing a fine basketweave of  $\alpha$  lamellar, Fig. 1(b). The basketweave structure was consistent throughout the microstructure with no evidence of single  $\alpha$  lamellar orientation clustering in the form of colonies. The average  $\alpha$  lamellar thickness was measured as 1.13  $\mu\text{m}$  and the volume fraction of  $\alpha$  and  $\beta$  was measured to be 55.60% and 43.30%, respectively.

The as-received material was face turned across the whole cross-section of the billet from edge to centre using a WFL M100 MillTurn CNC machining centre. To gather the machining force signals a Kistler 9129AA dynamometer was fitted to the machine tool head to collect the cutting force tangential to the rotation,  $F_C$ , the force in the feed (radial) direction,  $F_F$ , and the normal force in the longitudinal axis,  $F_L$ . Fig. 2 shows schematically the forces measured in the three spatial axes with respect the workpiece and tool holder (Fig. 2(a)) and with respect the tool insert (Fig. 2(b)).

Machining parameters selected were 0.1 mm depth of cut, 0.1 mm/rev feed per revolution, and 70 RPM rotation rate. The cutting tool insert used was a CNMG 12 04 08 SM 1115 manufactured by Sandvik. This insert has a tool nose radius of 0.8 mm, i.e., much greater than the depth of cut. A straight radial line was scribed on the workpiece face to act as a datum point to ensure that the data synchronisation methods used were performed correctly. The data acquisition rate per data collection channel was 4KHz, giving a data collection resolution of 100  $\mu\text{m}$  in the radial direction and a circumferential resolution of 107.2  $\mu\text{m}$  at the outer radius of 58.5 mm. At other radii, the circumferential resolution is increased by the ratio 58.5: R, where R is the instantaneous radius in mm. The machined chip produced was continuous with each segment having a length of at least 10000  $\mu\text{m}$ , much greater than the measured  $\beta$  grain size. The continuous nature of the chip minimised forces from chip formation vibrations and chip shearing, thus enhancing any potential microstructure features within the force signal.

The experimental machining parameters were chosen to minimise the tool-material interaction volume and chip/rake face friction forces to maximise the sensitivity of the cutting forces to microstructure. It should, however, be pointed out that the data from the three orthogonal forces being acquired represent different aspects of the machining process.  $F_C$  is dominated by the force required to separate the chip from the workpiece but because the cutting tool is rubbing on the new machined surface and the extended chip is making contact with the rake face of the tool, frictional components of force are also included in the  $F_C$  value. The chip/rake face interface frictional force is reduced by selecting a small depth of cut (0.1 mm) and a small feed rate (0.1 mm/rev feed per revolution) minimising the uncut chip thickness and hence the chip size and weight.  $F_F$  also has components of separation force and rubbing and chip/tool interface frictional forces. However, the chip/rake face forces are reduced owing to the small rake angle (15°) selected but the rubbing frictional forces are increased because of the extra downward force generated by the tool feed movement. The downward tool feed movement also adds an extra elastic force to  $F_F$ .  $F_L$ , on the other hand, is relatively simple mainly influenced by the contact (friction and elastic) between the tool insert and the newly as-machined surface.

## 3. Results

Fig. 3(a) shows the cutting force signals,  $F_F$ ,  $F_C$ , and  $F_L$ , for just over one rotation, with the large spike clearly identifying the scribed line, while Fig. 3(b) shows an example higher resolution  $F_L$  signal section covering 60ms. The average  $F_L$  and  $F_C$  forces are similar at just below 40 N, while the average  $F_F$  force is considerably lower at just above 10 N. The force fluctuations about the mean are greater for the  $F_L$  signal with a range of approximately 10N, while the fluctuations for  $F_L$  and  $F_C$  are approximately 5N. Thus, the force fluctuation range to average force ratios for  $F_F$ ,  $F_C$ , and  $F_L$  are approximately 0.25, 0.5, and 0.125, respectively. An attempt is also made in Fig. 3(b) to identify the size of the force signal fluctuations, which match closely with the average  $\beta$  grain size measurement.

Fig. 4(a)–(d) shows the force signal data gathered for the whole cross-section of the billet for all three force signals, plus the resultant force (Mag). The scribed radial line is visible and straight, confirming that the methodology to synchronise the data gathered as a function of time with spatial location is accurate. Furthermore, it is clear that local regions of higher and lower forces are being identified at the same loca-

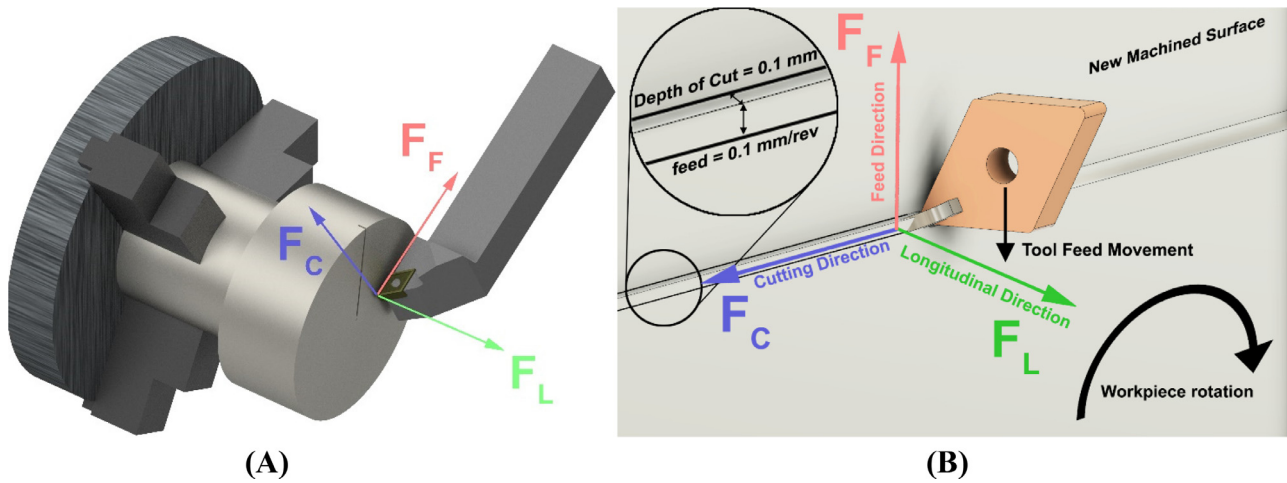


Fig. 2. (a) Representation of the force nomenclature with respect to the sensor-tool reference axis and (b) detail of the forces respect the insert (b) (Schematic not to scale).

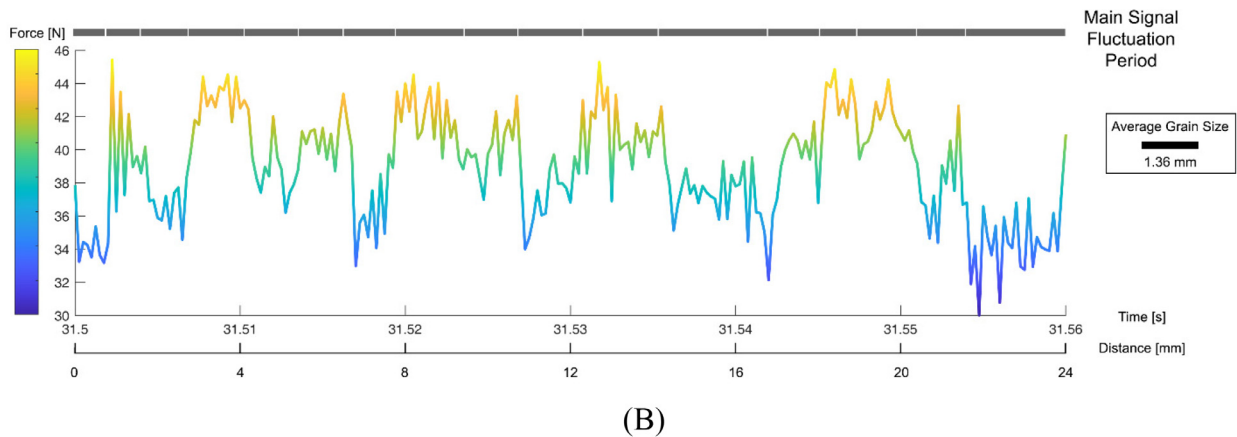
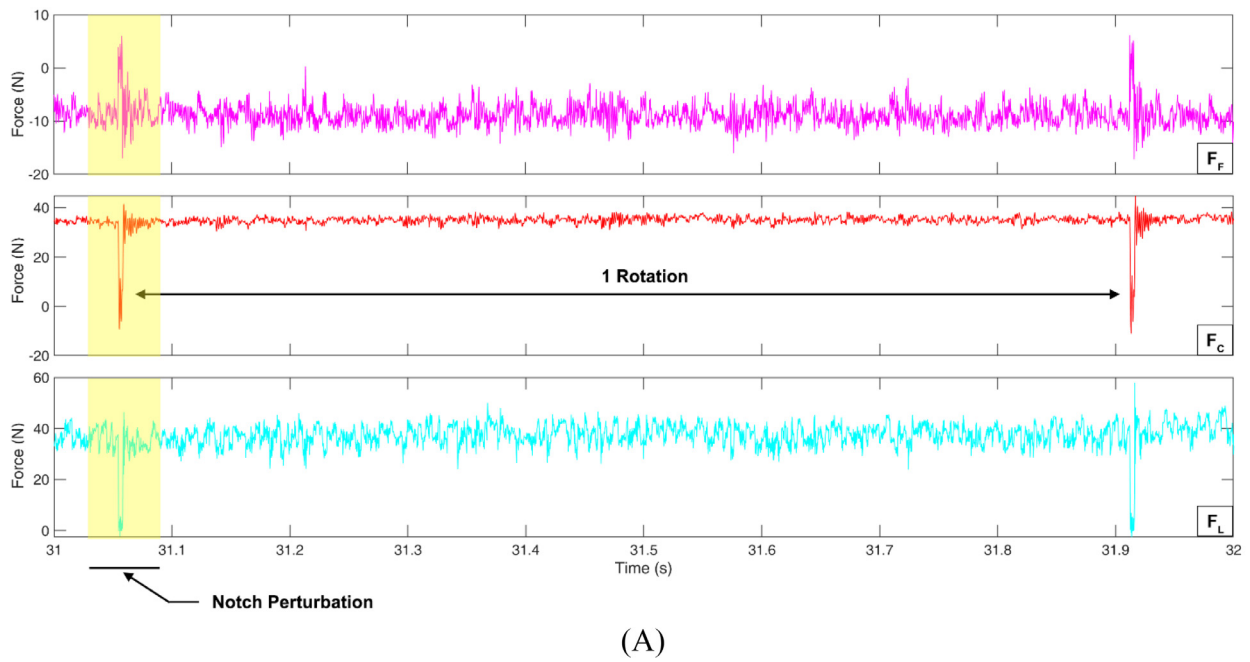


Fig. 3. Signals gathered through dynamometer. (a) Example of force signals collected through the dynamometer during a face turning operation  $F_C$ ,  $F_F$  and  $F_L$ . (b) 60ms of signal from  $F_L$  sensors and signal zones highlighted with individual microstructural units.

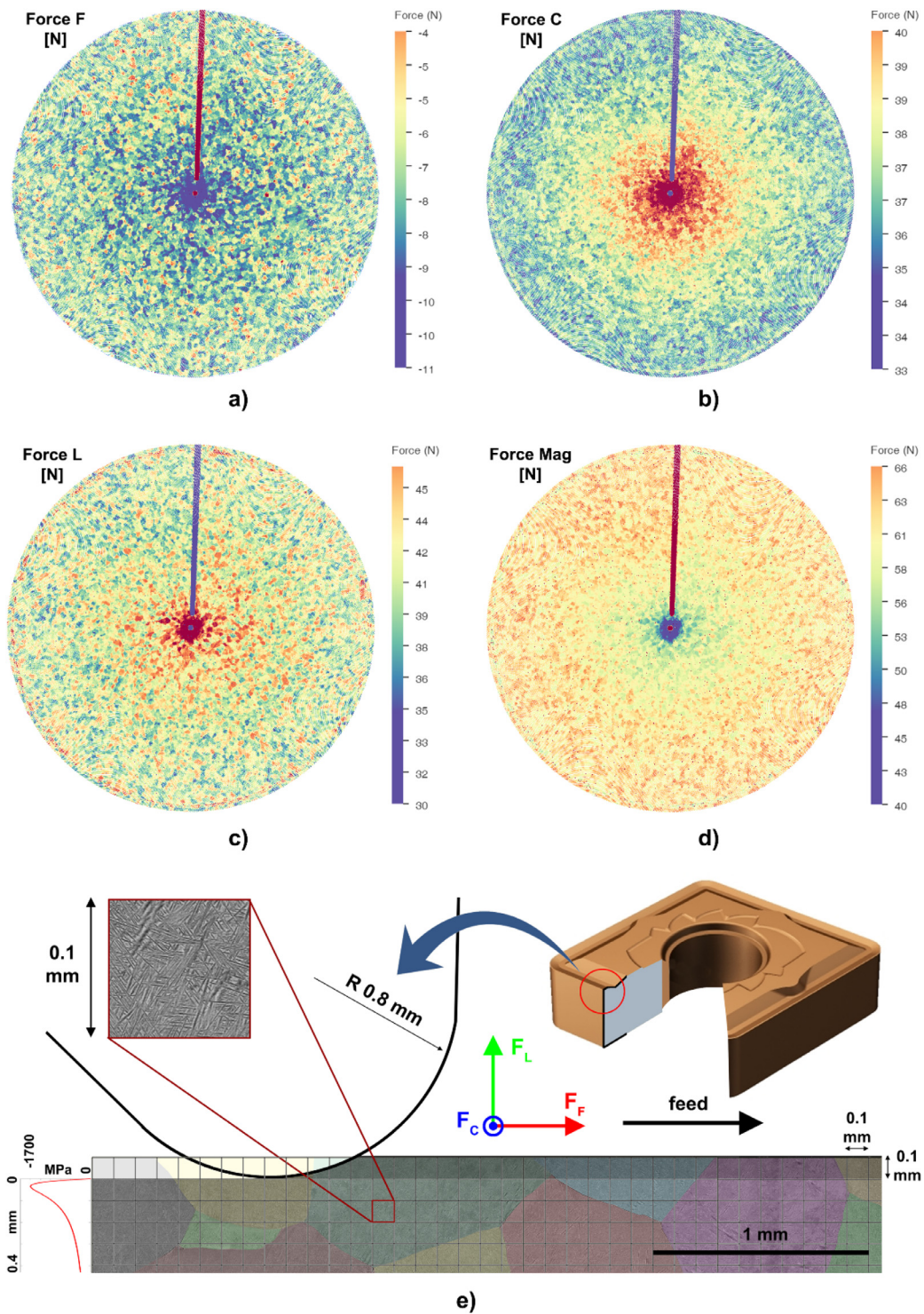


Fig. 4. Force feedback diagrams obtained from the dynamometer reading while performing the face turning operation of the 117mm billet. Feed Force [ $F_F$ ] (a), Cutting Force [ $F_C$ ] (b), Longitudinal Force [ $F_L$ ] (c), resultant module of the three axis combination forces (d). [Note,  $F_F$  has its scale inverted because of the location of the dynamometer axes with respect to the workpiece.] and (e) microstructure of machined Ti-17 billet with beta grains highlighted and tool radius at the same scale, detail of Widmanstätten acicular alpha laths in the analysed microstructure and force axes for reference. Hertzian pressure profile calculated is shown at the left in red.

tions are covering many data points both circumferentially and radially. As per Fig. 3(b), these high and lower force segment sizes again appear to match well with the  $\beta$  grain size.

It should be noted, that this test was undertaken using constant RPM conditions. This means the angular speed was kept constant while the cutting speed (or surface speed) decreases towards the centre. Thus, near

the centre of the test ( $R < 12.38$  mm) the lower cutting speed modifies machining conditions and chip formation mechanisms making the cutting forces higher.

Fig. 4(e) shows the microstructure of the machined billet with the  $\beta$  grains, highlighted in colours, superimposed with a schematic of the machine tool radius at the same scale as the microstructure. The over-

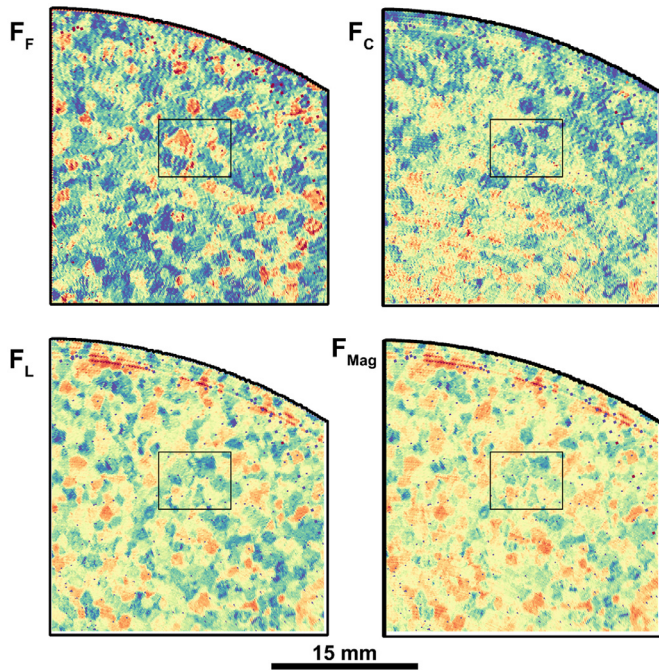


Fig. 5. Detailed image of the reconstructed fingerprint diagrams per axis and the reconstructed image using the resultant force value  $F_{Mag}$ , region of interest with different local machining signal per axis.

laid grid represents the depth of cut and feed resolution based on the machining parameters selected in the feed direction. To understand the interaction volume of the force signal with respect to microstructure features the contact pressure region was calculated using the theoretical Hertzian contact stress calculation [11]. Assuming the tool can be considered a cylinder and the maximum applied force is 70N, the maximum stress under this cylinder-plane interface occurs at a depth of  $45\mu\text{m}$  (see left hand side of Fig. 4(e)), meaning that the interaction volume is considerably smaller than the  $\beta$  grain size.

Considering the interaction volume as a 2D section of a cylinder with a diameter equal to the depth of the compressive stress equal to the yield strength and length equal to 0.176 mm, the interaction volume represents only 0.18% of the volume of an average grain, considering it spherical with diameter 1.36 mm. Clearly, this interaction volume is too large to capture any individual  $\alpha$  lamellas.

A further feature of Fig. 4 is that it appears that some different local heterogeneities are highlighted when constructing the force feedback diagrams with the different cutting force signals. For example, neighbouring local regions that are clearly distinguishable as two separate features when analysing with one of the signals (e.g.,  $F_F$ ) show similar or even identical machining behaviour when analysing with another signal (e.g.,  $F_L$ ). To illustrate these differences, a section of the machined cross-section of the billet is highlighted in a rectangle near the middle of the figures in Fig. 5. At the bottom left of the highlighted region in the  $F_F$  diagram there are two clear blue features, however, at the equivalent location in the  $F_L$  diagram there is more contrast, with more features highlighted, than what is shown in the  $F_F$  diagram. At the top right corner, a similar situation exists but in the opposite way with the two blue features in the  $F_L$  diagram having more contrast than in the  $F_F$  diagram. By combining the three forces into a single vector,  $F_{Mag}$ , it appears that more contrast is generated than a single force dataset, suggesting that the optimum microstructure capture most likely needs to incorporate information from all three orthogonal force measurements. Note, that the diagram created using the  $F_L$  signal and that constructed with the magnitude force ( $F_{Mag}$ ), are quite similar. This is because: 1. the magnitude of  $F_F$  is much smaller than either  $F_C$  or  $F_L$ , meaning its effect gets

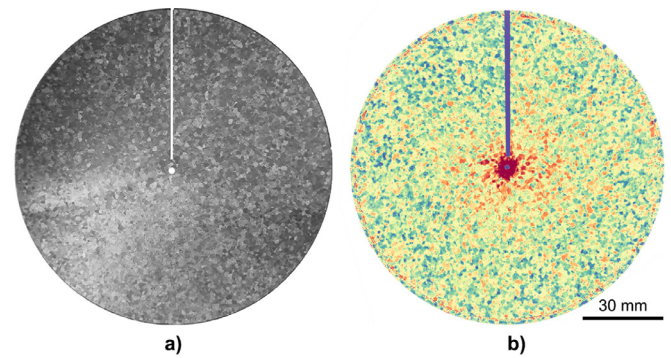


Fig. 6. Ti -17 billet etched surface of the billet after the machining operation (a), force feedback diagram with  $F_L$  signal (b).

washed out in  $F_{Mag}$ , and 2. The force fluctuation range in  $F_C$  is half that of the fluctuation range in  $F_L$ , meaning any information captured in  $F_C$  is not as impactful in comparison to  $F_L$  when combined to form  $F_{Mag}$ .

To determine how accurate the prediction of  $\beta$  grain size is using the force measurement technique presented, the as-machined billets were examined metallographically. The machined surfaces were etched in a solution of HF and lactic acid for a “dark etching” finish performed by Timet UK Ltd. A comparison between the  $F_L$  force feedback image and as-etched microstructure at low magnification is shown in Fig. 6, which appears to show a good correlation between the structural unit sizes being revealed by both techniques.

To increase the resolution and quality of the constructed image, and to have a one-to-one detailed comparison with the etched micrograph of the complete cross section, a mathematical treatment of the machining force signals was undertaken. First, all three axes were normalised before the calculation of the resultant force. This was performed to enhance the impact of the  $F_C$  signal and thus create a diagram with higher contrast between local machining fluctuations. The second stage was to perform signal filtering using a Fourier transform analysis, where a high pass filter cut off the effects occurring at more than 400Hz, reducing signal noise. Finally, a Kuwahara filter [12] was applied to the noise reduced image to enhance contrast between different regions that only have small differences in cutting performance, bringing a higher resolution to the boundaries between these regions. Fig. 7 shows the signal improvement through these filtering techniques compared to the etched image, Fig. 7(a), and the original  $F_L$  signal, Fig. 7(b). Fig. 7(c) shows the detail of the microstructure reconstructed using the normalised  $F_{Mag}$  data, which shows improved contrast between microstructure features in comparison to the diagram created using the single axis  $F_L$  data. Fig. 7(d) shows the normalised and noise reduced  $F_{Mag}$  data after Kuwahara filter refinement, which has created an image with a similar level of contrast to the etched material in Fig. 7(a). It should also be noted that there was significant improvement in visualisation of the new  $F_{Mag}$  image when plotted as greyscale, and thus subsequently all images were converted to greyscale.

Grain size measurements using the linear intercept method were undertaken on both the as-etched and the new optimised  $F_{Mag}$  image at equivalent locations, as shown in Fig. 8. There appears to be a good level of correlation between the two sets of data with the maximum difference between any of the lines measured being 5%, suggesting it is possible to perform quantitative grain size data analysis directly from machining force feedback.

#### 4. Discussion

The results presented above have demonstrated a close correlation between the local force fluctuations measured during machining and the beta grain size of Ti-17, as measured using standard etching techniques. This confirms the previous hypothesis of Crawford et al. [6] that local

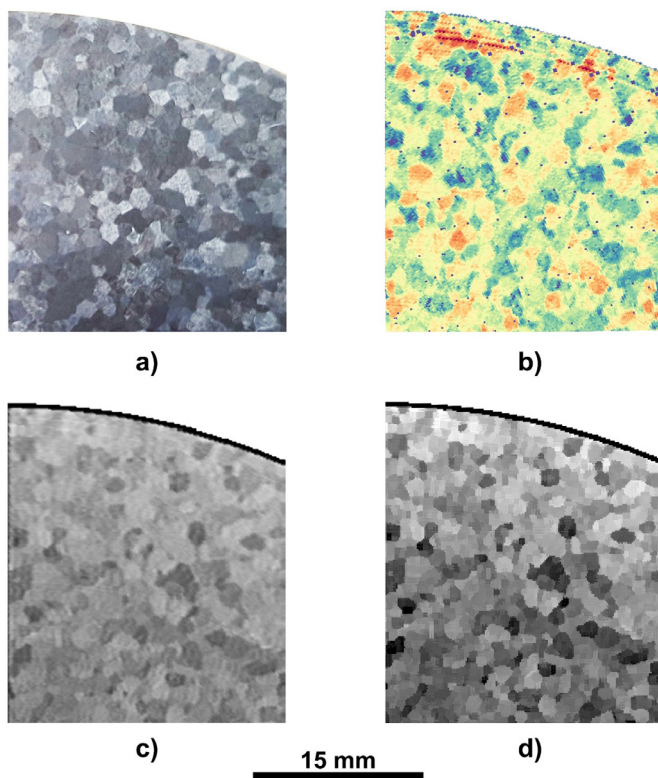


**Fig. 7.** Region detail of the machined titanium billet. (a) Detail of the etched microstructure, (b) fingerprint reconstruction using original  $F_L$  signal, (c) fingerprint reconstruction using the new normalised resultant force,  $F_{Mag}$ , showing enhanced information and contrast and (d) Kuwahara filtered fingerprint  $F_{Mag}$  diagram of the same region highlighting regions and grain boundaries for close comparison.

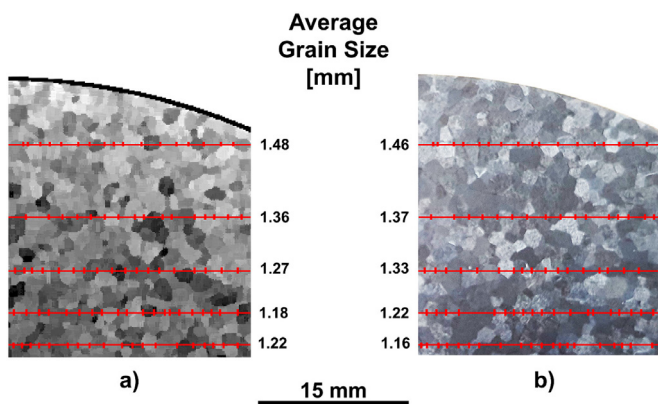


**Fig. 8.** Equivalent location grain size measurement performed in equivalent location in the (a) reconstructed normalised and filtered signal fingerprint and (b) the etched image detail.

machining heterogeneities could be linked to the microstructure characteristics found within the component. However, several signal conditioning steps are required to gain data with sufficient fidelity to enable quantitative analysis. In the first instance, it was found that each force signal did not capture the complete spectrum of microstructure features and that each signal captured slightly different elements of microstructure information. This was overcome by combining the microstructure information of all three forces into a single resultant force vector, which required the normalisation of the raw forces because of the large differ-

ences in their magnitude. The resultant force was then mathematically treated using a Fourier transform for reduction of high frequency noise that could be attributed to either external influences, such as system vibration or to microstructure features on a much finer scale, such as individual  $\alpha$  lamellar. The resultant image was then adaptively noised reduced by using the Kuwahara filter to enhance grain boundary detection. This resulted in an image, Fig. 7(c), that closely resembled the same area when chemical etched, Fig. 7(d), suggesting the proposed methodology has potential as an in-situ technique of microstructure characterisation.

The measured cutting forces are a function of the material's elastic and plastic behaviour within the interaction volume in combination with friction effects and the local fracture behaviour. Therefore, owing to the interaction volume being less than the  $\beta$  grain size but much greater than individual  $\alpha$  lamella it is not unreasonable to assume that the forces being measured are a function of the individual orientation of the  $\beta$  grain plus a contribution from the  $\alpha$  lamellas. However, it is unclear if the  $\alpha$  lamellas are adding an average increase or decrease to the  $\beta$  grain forces or an orientation specific force owing to the Burgers orientation relationship between  $\beta$  and  $\alpha$ . If it is the latter, there may potentially be a greater grain to grain variation because of the anisotropy of the hcp crystal of the  $\alpha$ . However, Zhang et al. [13] showed for Ti-17 with a similar basketweave morphology, but with thicker lamella, that at least 7  $\alpha$  orientation variants are formed within a  $\beta$  grain. This leads to the conclusion that the  $\alpha$  contribution to the overall machining force contribution is most likely linked to an average crystallographic response, rather than a specific crystallographic orientation. For other titanium alloys where this is a more colony like microstructure [14] where there is a clustering of similarly orientated  $\alpha$  lamella at potentially the size of the interaction volume, the structural units being detected may, in fact, be the colony or be heavily influenced by the colony orientation.

Chip formation forces and the friction exerted on the tool are a function of the rake face angle of the used insert. Considering a small positive rake angle ( $15^\circ$  in this case), most of the chip formation force and its friction over the tool is represented in the  $F_F$  and  $F_C$  axes. Moreover, owing to the small depth of cut and feed parameters selected, these effects are further minimised. However,  $F_L$  is affected by the pressure exerted in the as-machined wall, i.e., the plane perpendicular to the rotational axis. Although no material removal occurs in this edge of the cutting tool, the constant friction and pressure of the tool smearing the surface, provides an elastic response of the material in this axis without inducing any plastic deformation. It is, therefore, interesting that  $F_L$  and  $F_C$ , which have a higher proportion of elastic response in their total values produced the higher contrast images, as shown in Fig. 5, suggesting that elastic stresses produce the highest contrast between grains and plastic strains smear out the grain to grain variation.

Future work for this technology will be centred on the analysis of other types of alloys and microstructures, as well as the study of the effects of different forging processing routes and heat treatments on the force feedback diagrams. Further signal analysis and filtering will also allow for improving the machining processes by modifying the local machining parameters in-situ, such as the cutting speed, to achieve the highest quality and best performance possible from an as-machined component. A flow chart explaining this concept is shown in Fig. 9(a), where the information gathered during the machining operation can be analysed and through the understanding of the relationship between force feedback and final component's performance, a new more suitable cutting speed can be calculated and implemented, assuring quality levels. Moreover, this analysis technique provides unique information from the machined sample that can be used for accepting or discarding samples, as an NDT process, while performing the machining operation. This is shown in Fig. 9(b). This could be implemented as an extra safety measure, where if a certain force value is registered at any point of the machined surface, the component can be automatically discarded from earlier production stages, making more efficient use of resources.

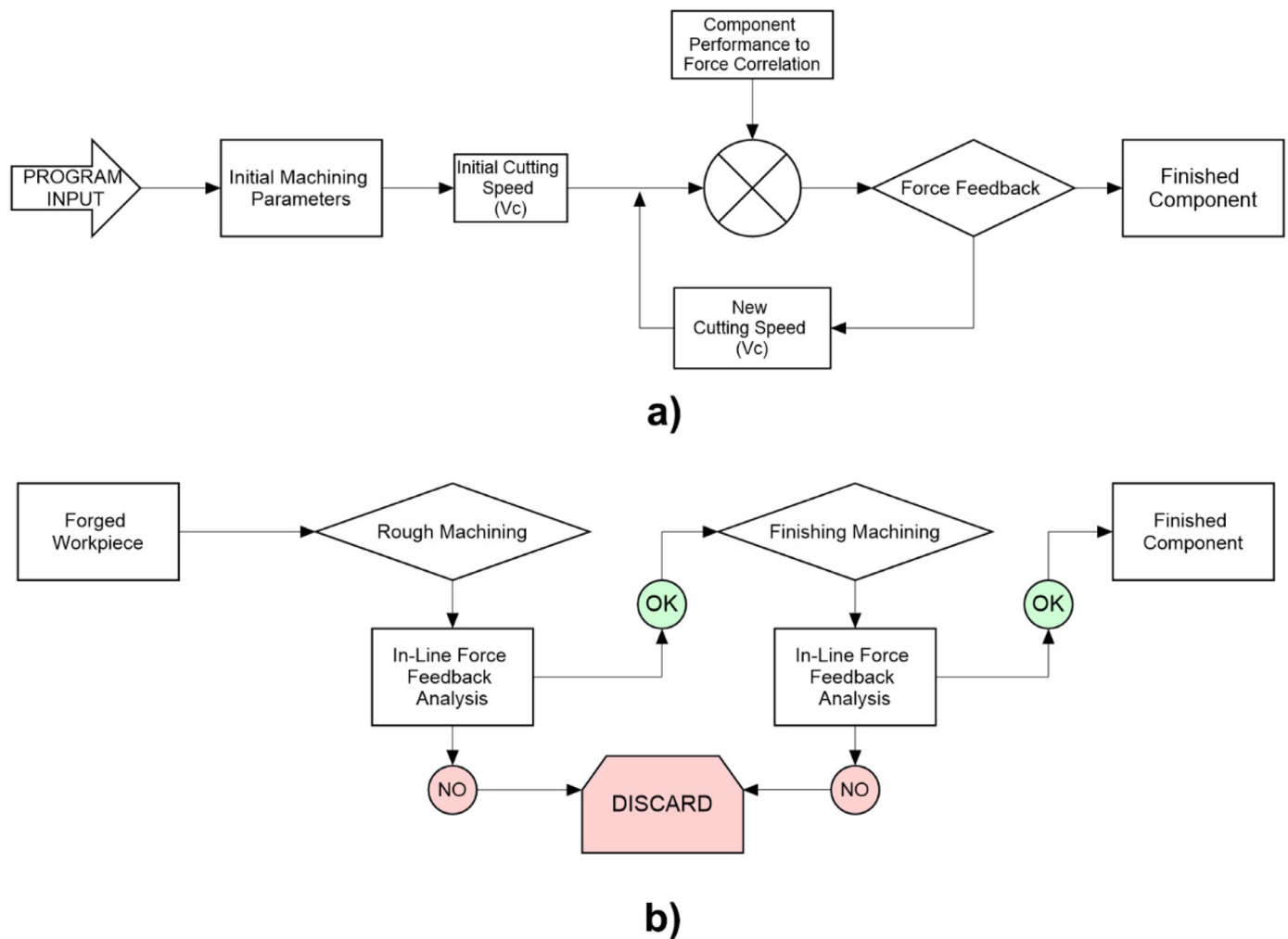


Fig. 9. (a) Potential application for in-situ analysis and local tailor machining parameters (in this case cutting speed) based on the force feedback response from the underlying microstructure and (b) flowchart of in-line validation of components for a standard roughing and finishing machining processes.

## 5. Conclusion

The fluctuating forces on the cutting tool generated during machining of  $\beta$  processed Ti-17 alloy have been shown to contain sufficient information to enable measurement of  $\beta$  grain size to an equivalent resolution of standard etching methods. To gain an image of high enough resolution to measure grain size, the orthogonally measured forces required noise reduction and had to be normalised and combined into a resultant force vector to capture the slightly different microstructure sensitivity of each force measurement. Moreover, the forces that have a larger elastic component, i.e.,  $F_L$  and  $F_F$ , appear to be more microstructure sensitive as they produce higher contrast individual images than the cutting force,  $F_C$ , which has a large component of plastic deformation and separation forces in it. This suggests that a small depth of cut and feed per revolution, which enhance the ratio of elastic to plastic deformation, will generate a higher contrast microstructure image and thus more accurate grain size analysis.

## Declaration of Competing Interest

The authors declare that they have no known competing financial interests or personal relationships that could have appeared to influence the work reported in this paper.

## Acknowledgments

We would like to acknowledge Dr. Ben Thomas for helping with the data handling aspect of this research and graphics creation, and Dr. Mathew Thomas and Timet UK Ltd. for supply of materials.

DSF would also like to thank Rolls-Royce Plc. and The Engineering and Physical Science Research Council (UK) through the Centre for Doctoral Training in Advanced Metallic Systems (EP/L016273) for supporting this research.

## References

- [1] A.F. Wilson, V. Venkatesh, R. Pather, J.W. Brooks and S.P. Fox, Proceedings for the Tenth Conference in Titanium (2003) vol. 1, 321–328.
- [2] P S Davies, B.P. Wynne, M.J. Thomas, W.M. Rainforth, IOP Conf. Ser.: Mater. Sci. Eng. (2017) 375.
- [3] J. Xie, M.J. Luo, K.K. Wu, L.F. Yang, D.H. Li, Experimental study on cutting temperature and cutting force in dry turning of titanium alloy using a non-coated micro-grooved tool, Int. J. Mach. Tools Manuf. 73 (2013) 25–36.
- [4] W. Pan, S. Ding, J. Mo, The prediction of cutting force in end milling titanium alloy (Ti6Al4V) with polycrystalline diamond tools, Proc. Inst. Mech. Eng. B: J. Eng. Manuf. 231 (1) (2017) 3–14.
- [5] S.L.M.R. Filho, R.B.D. Pereira, C.H. Lauro, Investigation and modelling of the cutting forces in turning process of the Ti-6Al-4V and Ti-6Al-7Nb titanium alloys, Int. J. Adv. Manuf. Technol. 101 (2019) 2191–2203.
- [6] P Crawford, M. Jackson, S. Turner and B.P. Wynne, Proceedings of the Thirteenth World Conference on Titanium, TMS, (2016), 1649–1654.
- [7] Z. J. Yuan, Y.X. Yao and M. Zhou, Effect of crystallographic orientation on cutting forces and surface quality in diamond cutting of single crystal CIRP annals (1994) Vol. 43, Issue 1, 39–42

- [8] B.L. Lawson, N. Kota, O.B. Ozdoganlar, Variation of cutting forces in machining of f.c.c. single crystals, *J. Manuf. Sci. Eng.* 130 (3) (2008) 1–11 031116.
- [9] W.B. Lee, S. To, C.F. Cheung, Effect of crystallographic orientation in diamond turning of copper single crystals, *Scr. Mater.* 42 (2000) 937–945.
- [10] Timet Ltd. Ti-17 Commercial Composition range.
- [11] R.G. Budynas, J.K. Nisbett, *Shigley's Mechanical Engineering Design*, 9th ed., McGraw-Hill Higher Education, 2011.
- [12] M. Kuwahara, K. Hachimura, S. Eiho, M. Kinoshita, Processing of RI-angiocardio-graphic images, in: K. Preston, M. Onoe (Eds.), *Digital Processing of Biomedical Images*, Springer, Boston, MA, 1976.
- [13] S. Zhang, W. Zeng, Q. Zhao, L. Ge, M. Zhang, In situ SEM study of tensile deformation of a near- $\beta$  titanium alloy, *Mater. Sci. Eng. A* 708 (2017) 574–581.
- [14] G. Lütjering, J.C. Williams, *Titanium*, Springer-Verlag, Berlin Heidelberg, 2003 ISBN 978-3-662-13222-7.